MODELING OF DISSOLUTION TRANSPORT OF NONAQUEOUS PHASE LIQUID WASTES IN HETEROGENEOUS AQUIFERS

S. Okeson, T.H. Illangasekare, D.C. Szlag and J.E. Ewing, Department of Civil, Environmental and Architectural Engineering, University of Colorado, Boulder, CO 80309-0428

ABSTRACT

A two-dimensional dissolution experiment was conducted to examine the influence of dimensionality and rate-limited mass transfer on the dissolution of an entrapped, multicomponent nonaqueous phase liquid. A synthetic gasoline mixture entrapped below the water table in a coarse gravel lens provided a source zone of benzene. Downgradient aqueous concentrations gave insight on the dissolution process at both high organic saturation and at residual organic saturation after the free product was recovered. Modeling of the system was undertaken using a decoupled approach. The ground water flow field was established first, then a solute transport model incorporating a rate-limited dissolution term was used to describe the dissolution and transport of benzene from the entrapped nonaqueous phase mixture.

KEY WORDS

nonaqueous phase liquids, dissolution, ground water

INTRODUCTION

Some of the most common releases of organic chemicals in the environment, i.e., gasoline and jet fuel, do not consist of a single component, but are lighter-than-water nonaqueous phase liquids (LNAPLs) composed of many water immiscible and partially miscible organic constituents. Previous work has shown LNAPLs may be immobilized by differences in fluid entry pressure at boundaries of physical heterogeneities, resulting in entrapment saturations that are much larger than residual. These macroscale-entrapped LNAPLs may be present at very high saturations, even below the water table [1-3]. These entrapped LNAPL bodies are difficult to mobilize and may be long-term sources of ground water pollution. This work examined the applicability of modeling mass transfer from a macroscale-entrapped LNAPL body to flowing water with a lumped mass transfer coefficient and a linear driving force.

THEORY

Dissolution of NAPLs is a complex phenomena. It is commonly assumed that the system is at local equilibrium in the region of entrapped NAPL and that water emanating from source zones is at maximum aqueous concentration. However, limitations on mass transfer between phases may prevent the system from establishing equilibrium aqueous concentrations. NAPL concentration differences, interfacial area and local ground water velocity may all play a part in controlling the rate of mass transfer from the NAPL phase to the bulk aqueous phase. These complexities may be handled by combining the many factors controlling mass transfer into a lumped mass transfer rate coefficient, k. Several researchers [4-6] have presented dimensionless correlations relating mass transfer to flow system parameters.

Szlag [6] suggests that the rate of mass transfer from macroscale-entrapped NAPLs

Figure 1. Schematic of the large aquifer flume.
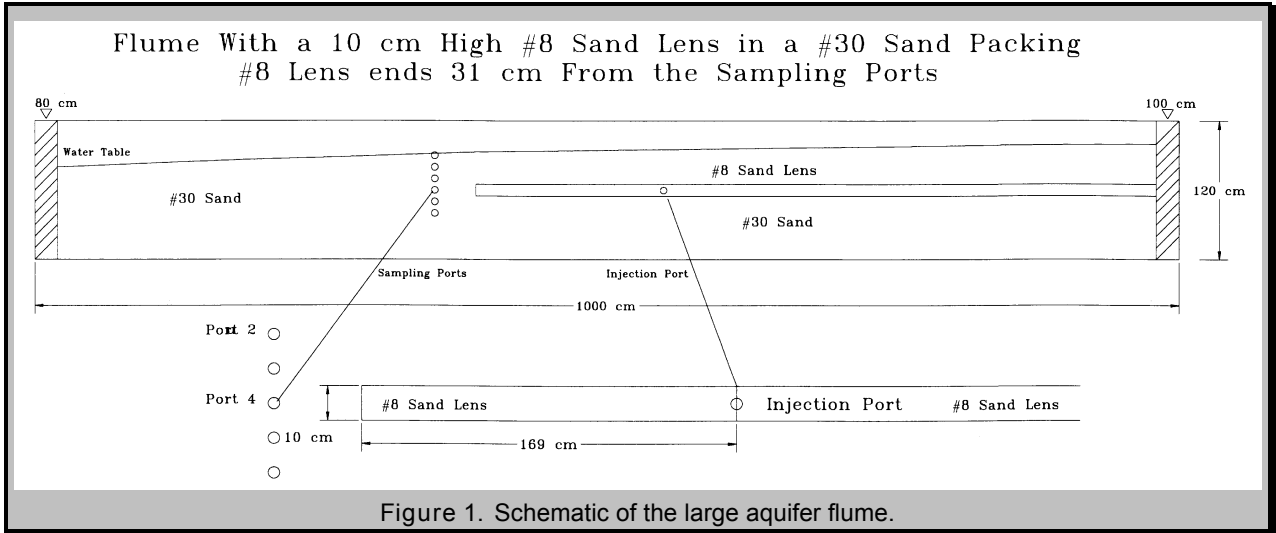
is particularly dependent on the rate of water velocity through the NAPL source zone. Szlag proposed a dimensionless Gilliand-Sherwood correlation of the form:

$$Sh^* = \alpha Re^{\beta} \qquad (1)$$

with α and β being constants ($\alpha = 11.2$ and $\beta = 0.63$ for dissolution experiments conducted by Szlag [6] for p-xylene). Table 1 describes the dimensionless groups. This correlation was incorporated into a solute transport code, MT3D [7], and used to model the dissolution experiment.

EXPERIMENTAL PROCE-DURES

Differences in capillary pressure of the non-wetting phase (NAPL) and the wetting phase (water) must exceed some finite value, called entry pressure, for the non-wetting fluid to displace the wetting fluid in a porous media [8]. Changes in entry pressure may trap NAPLs at porous media interfaces. This concept was utilized to hold a synthetic gasoline mixture below the water table, creating a source for the dissolution experiment.

A simplified physical environment simulat-

Reynolds Number	$Re = \dfrac{\rho_w d q_w}{u_w}$	Inertial Forces / Viscous Forces
Modified Sherwood Number	$Sh^* = \dfrac{k d^2}{D_m}$	Mass Transport / Diffusive Forces

where subscript w is the water phase

ρ is the density [$M\ L^{-3}$]

u is the viscosity [$M\ L^{-1}\ T^{-1}$]

d is the characteristic length (mean grain diameter) [L]

q is the Darcy velocity [$L\ T^{-1}$]

D_m is the molecular diffusion coefficient [$L^2\ T^{-1}$]

k is the mass transfer rate coefficient [T^{-1}]

Table 1. Relevant dimensionless groups.

ing possible field geology was established using a coarse sand lens inside a finer sand matrix in a vertical aquifer flume. A schematic of the experimental apparatus is shown in Figure 1. A NAPL mixture (total volume of 1414 ml, 10% benzene, 74% cyclohexane, 16% 1-iodoheptane by weight) was injected into the coarse sand lens at a rate of 17.6 ml/min. The NAPL migrated downgradient before becoming entrapped at the end of the lens. Fifty hours after the initiation of the NAPL injection, a well was placed in the end of the coarse sand lens and 75% (by volume) of the NAPL recovered. The experiment continued for 100 hours after the NAPL recovery.

Aqueous samples were taken at five sample ports, 31 cm downgradient from the end of the lens and perpendicular to the ground water flow direction. The vertical spacing between ports was 10 cm, and port 4 was on the horizontal centerline of the #8 sand lens. Five hypodermic needles were sealed into the Plexiglas flume wall, with the hub of each needle connected to a plastic Luer valve. The needles were purged with 0.2 ml of flume water using a tuberculin syringe and a sample of 0.4 ml was then taken. The samples were placed in 5.0 ml glass vials containing 4.5 ml of deionized water. Sample benzene concentrations were determined by direct aqueous injection into a gas chromatograph equipped with a FID detector. External standards were prepared from water saturated with benzene. All benzene concentration data were reported in terms of relative benzene concentration, i.e., the ratio of benzene in the samples to standards that were prepared from water saturated with benzene (C/Cs).

NUMERICAL MODELING

This experiment represented a multiphase flow problem because of the mobile LNAPL during and immediately after the injection and following the recovery phase. The modeling effort did not attempt to handle the movement of the mobile NAPL; instead the modeling was directed at capturing the dissolution behavior during the period the #8 sand lens was at a high organic saturation, before the recovery phase.

A decoupled approach was used for the dissolution modeling. The ground water flow field was established using MODFLOW [9], a three-dimensional, finite difference ground water model supported by the United States Geological Survey. Based on the relative permeabilities experimentally determined by Szlag [6] for p-xylene, reduced hydraulic conductivities were assigned to the cells with NAPL present.

Amounts of NAPL were then assigned to individual cells for the dissolution modeling based on saturations determined by gamma spectroscopy. This modeling used a modified module in the solute transport code MT3D [7]. Under equilibrium conditions the distribution between the NAPL and aqueous phases may be described by

$$K_p = \frac{w}{C} \qquad (2)$$

where

ω	is the weight fraction of soluble NAPL in the NAPL phase [M M^{-1}]
K_p	is the NAPL partition coefficient [L^3 M^{-1}]
C	is the contaminant concentration in the aqueous phase [M L^{-3}]

For a single component NAPL, the partition coefficient is the inverse of the solubility of the NAPL in water. An equilibrium relative concentration (C/Cs) of 0.21 for benzene was experimentally determined by batch experiments for the LNAPL mixture.

A conceptual two "film" environment was used to describe a rate-limited dissolution scenario. A film of stagnant water immediately surrounding the NAPL is assumed to be at instantaneous equilibrium with the
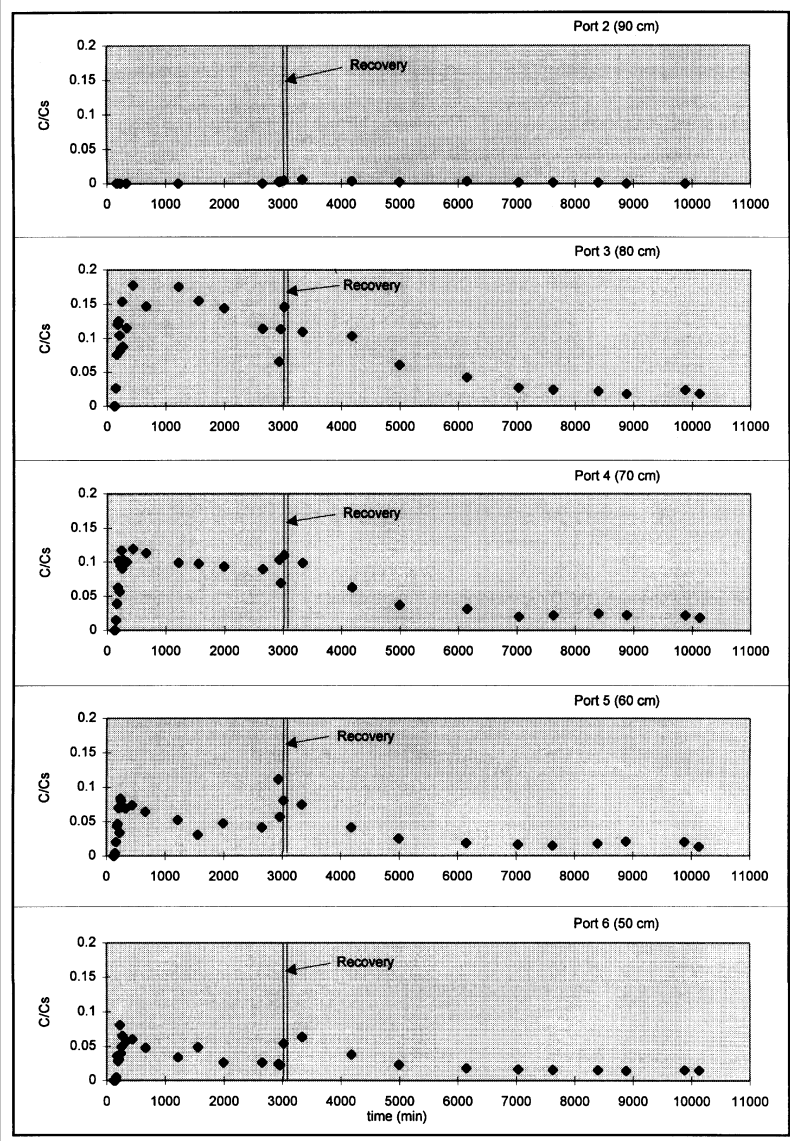
Figure 2. Measured aqueous benzene relative concentrations.

NAPL phase. This is determined by rearranging Equation 2:

$$C_{film} = \frac{w}{K_p} \qquad (3)$$

Mass transfer from this film to the bulk aqueous phase is rate limited. It is assumed this may be adequately described by a linear driving force model. The change in the bulk aqueous concentration in the cell is determined by:

$$\Delta C_{aqueous} = K(C_{film} - C_{aqueous})\Delta T \qquad (4)$$

where

K   is the lumped mass transfer rate coefficient (T^{-1})

The necessary mass of benzene is computed and subtracted from the NAPL phase for that cell. This has the effect of lowering the weight fraction of soluble benzene for a NAPL mixture and reducing the future
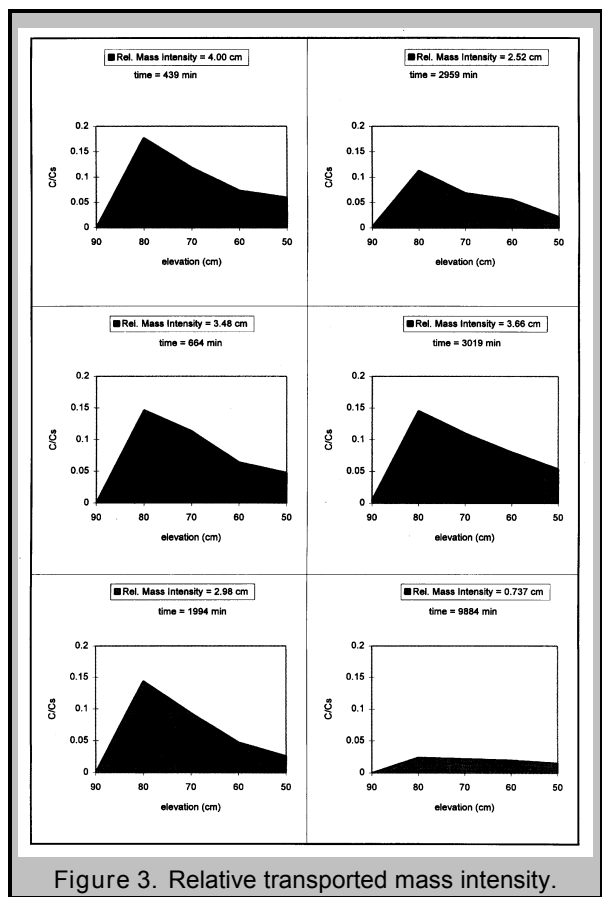
Figure 3. Relative transported mass intensity.

mass flux rate from that cell. These computations are done each transport step.

The basic models, MODFLOW [9] and MT3D [7] are publicly available by disk exchange from the Center for Subsurface Modeling Support in Ada, OK, and the modifications necessary for the incorporation of a dissolution term are freely available from the authors.

EXPERIMENTAL RESULTS

The experimental results are illustrated in Figures 2 and 3. The aqueous benzene concentrations declined over time, as the weight fraction of benzene in the source zone decreased. The highest aqueous concentrations in the flume were at port 3, five cm above the coarse sand lens and decreased in lower sampling ports. None of the samples reached the maximum relative benzene concentrations of 0.21 determined

from the batch experiments. The benzene concentrations increased after the recovery of the free product and then declined at a more rapid rate than before the recovery.

MODELING RESULTS

The large flume is a problematic modeling exercise. The NAPL is mobile for the first part of the experiment, resulting in a relatively large exposed NAPL surface area and a large amount of benzene transferred to the aqueous phase. The modeling attempted to capture the phase of the experiment once the NAPL was immobilized at the end of the coarse sand lens. This approach neglects the depletion of benzene from the NAPL that occurred at the start of the experiment. The simulation captured the trend of the breakthrough curves, but overpredicted the aqueous concentrations at port 4, directly downgradient of the lens, and underpredicted at port 3, 5 cm above the lens. The results for each port are shown in Figure 4.

DISCUSSION

The dissolution experiment demonstrated interesting behavior. The higher aqueous concentrations above the source were unexpected. This appears to be due to divergent water flow from the top of the source zone, caused by the reduced permeability of the source zone.

The increase in aqueous concentrations in the large flume after the NAPL recovery may be attributed to the exposure of "fresh" (less depleted of benzene) NAPL to the flowing water. The removal of a large volume of the entrapped NAPL increased the relative permeability of the NAPL source, allowing more water to flow through the source. The relative mass of benzene transported from the source increased after the recovery phase, and the benzene was more evenly distributed across the sampling array as seen in Figure 3.
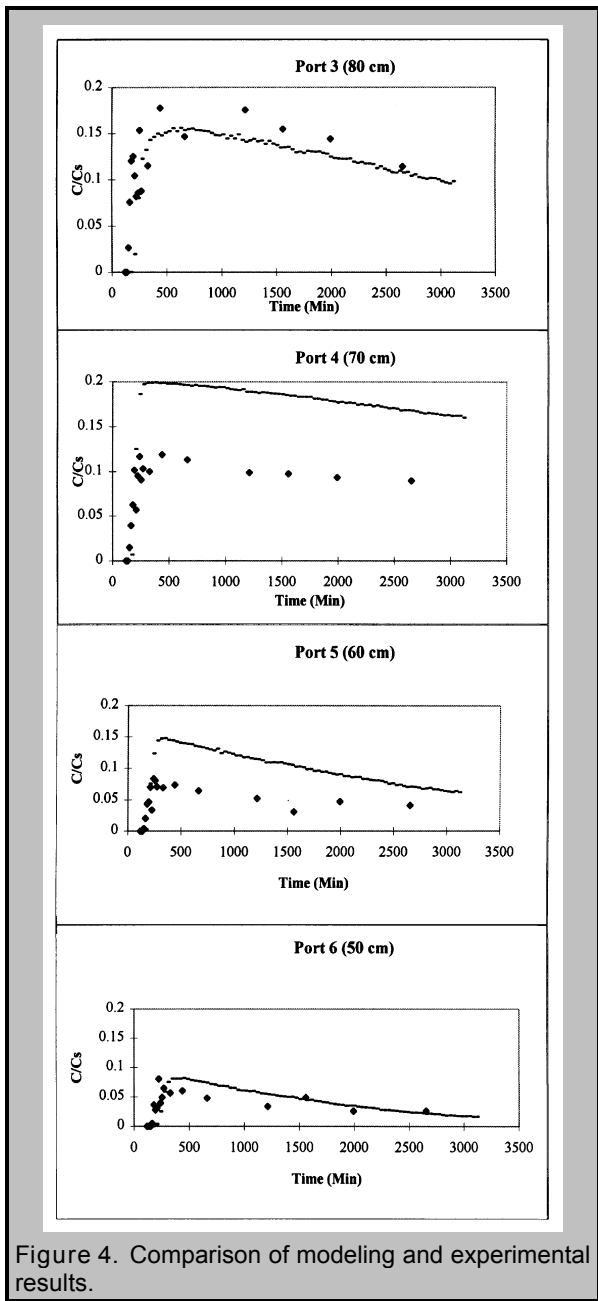
Figure 4. Comparison of modeling and experimental results.

CONCLUSIONS

The dimensionality of the experiment reduced the flux of benzene from the NAPL source due to water bypassing the source zone. This resulted in uneven depletion of benzene from the NAPL mixture. For an experiment run over a longer time scale, the diffusion of benzene within the NAPL mixture may have provided a limiting factor

to the decrease in aqueous benzene concentrations.

The model captured the trend of the large flume dissolution experiment over the time-scale that was simulated. Discrepancies in the experimental and model results are probably attributable to errors in the modeled flow field. The modeling methodology may be extended to test other dimensionless correlations for mass transfer from entrapped NAPLs to moving water.

ACKNOWLEDGMENTS

REFERENCES

1. T.H. Illangasekare, J.L. Ramsey, K.H. Jensen and M. Butts, Experimental Study of Movement and Distribution of Dense Organic Contaminants in Heterogeneous Aquifers, Journal of Contaminant Hydrology (In Press).

2. T.H. Illangasekare, D.N. Yates and E.J. Armbruster, Effect of Heterogeneity on Transport and Entrapment of Nonaqueous Phase Waste Products in Aquifers: An Experimental Study, ASCE Journal of Environmental Engineering, 121(8) (1995) 571-579.

3. D.A. Vroblesky, J.F. Robertson and L.C. Rhodes, Stratigraphic Trapping of Spilled Jet Fuel Beneath the Water Table, Ground Water Monitoring & Remediation (Spring 1995) 177-183.

4. T.C. Miller, M.M. Poirier-McNeill and A.S. Mayer, Dissolution of Trapped Nonaqueous Phase Liquids: Mass Transfer Characteristics, Water Resources Research, 26 (1990) 2783-2796.

5. S.E. Powers, L.M. Abriola and W.J. Weber, An Experimental Investigation of Nonaqueous Phase Liquid Dissolution in Saturated Subsurface Systems: Steady State Mass Transfer Rates, Water Resources Research, 28 (1992) 2691-2705.

6. D. Szlag, Dissolution of Trapped Waste Chemicals, Ph.D. Dissertation, University of Colorado at Boulder, 1995 (in preparation).

7. C. Zheng, MT3D: A Modular Three-Dimensional Transport Model for Simulation of Advection, Dispersion, and Chemical Reactions of Contaminants in Groundwater Systems, Prepared for US EPA Robert S. Kerr Environmental Research Laboratory, Ada, OK 74820, 1990.

8. A.T. Corey, Mechanics of Immiscible Fluids in Porous Media, Water Resources Publications, Littleton, CO, 1986, p. 255.

9. M.G. McDonald and A.W. Harbaugh, A Modular Three-Dimensional Finite-Difference Ground-Water Flow Model, Techniques of Water-Resources Investigations of the United States Geological Survey, Book 6: Modeling Techniques, 1988.